ORIGINAL ARTICLE

A Quantitative Systems Physiology Model of Renal Function and Blood Pressure Regulation: Model Description

KM Hallow* and Y Gebremichael

Renal function plays a central role in cardiovascular, kidney, and multiple other diseases, and many existing and novel therapies act through renal mechanisms. Even with decades of accumulated knowledge of renal physiology, pathophysiology, and pharmacology, the dynamics of renal function remain difficult to understand and predict, often resulting in unexpected or counterintuitive therapy responses. Quantitative systems pharmacology modeling of renal function integrates this accumulated knowledge into a quantitative framework, allowing evaluation of competing hypotheses, identification of knowledge gaps, and generation of new experimentally testable hypotheses. Here we present a model of renal physiology and control mechanisms involved in maintaining sodium and water homeostasis. This model represents the core renal physiological processes involved in many research questions in drug development. The model runs in R and the code is made available. In a companion article, we present a case study using the model to explore mechanisms and pharmacology of salt-sensitive hypertension.

Study Highlights

WHAT IS THE CURRENT KNOWLEDGE ON THE TOPIC?
☑ The kidney plays a central role in many diseases and therapies, but the complexity of renal function makes understanding and predicting therapy effects challenging.
WHAT QUESTION DID THIS STUDY ADDRESS?
☑ We present a model of renal physiology that facilitates dynamic simulation of renal and systemic hemodynamics. The model runs in R and the code is made available.
WHAT THIS STUDY ADDS TO OUR KNOWLEDGE
☑ The model presented here incorporates key processes and feedback mechanisms important for many research questions in renal drug development, and thus provides a core model that can serve as the starting point for a wide range of modeling endeavors.
HOW MIGHT THIS CHANGE DRUG DISCOVERY, DEVELOPMENT, AND/OR THERAPEUTICS?
☑ This model provides a platform that may facilitate evaluating the renal response to potential targets in development, identifying patient subgroups most likely to benefit from a treatment (or subgroups who may be harmed), simulating and interpreting of counterintuitive biomarker data related to renal function and/or renal toxicity, and relating preclinical and short-term clinical biomarkers to long-term responses and outcomes.

Renal function is central to many diseases, including hypertension, chronic kidney disease, and heart failure. Most drugs that effectively treat these diseases act through renal mechanisms. A large body of knowledge and data about renal physiology, pathophysiology, and pharmacology has been generated over decades from studies in humans and animals, in health and disease, over timescales from minutes to decades, using a variety of interventions, measuring a variety of biomarkers. But even with all of this information, understanding and predicting renal function and the renal response to therapy remains challenging. The multiple feedback systems involved over different timescales and interaction with the larger cardiovascular system can produce counterintuitive behavior and make it difficult to integrate all these pieces of data into a full picture of renal function.

Mathematical modeling provides a means for integrating accumulated knowledge and data into a consistent quantitative framework, allowing evaluation of competing hypotheses, identification of knowledge gaps, and generation of new hypotheses. Such models have many applications in drug development: quantitative evaluation of the renal response to potential targets in development, identifying patient subgroups most likely to benefit (or suffer) from treatment, interpreting counterintuitive biomarker data, and relating preclinical and short-term renal biomarkers to long-term responses and outcomes.

Regardless of the application, many of the core renal physiological processes involved are the same. Thus, a core model of renal function may be applied in a wide range of modeling endeavors, while also serving as a data integration tool that can be improved over time as it is tested, refined, and informed with additional data. This process could extend across research groups in both industry and

University of Georgia, Athens, Georgia, USA. *Correspondence to: KM Hallow (hallowkm@uga.edu)

academia, and both preclinical and clinical applications. However, this requires the establishment of a core model to serve as a starting point.

The field of renal mathematical modeling is not new—it was initiated in the 1970s by Arthur Guyton and Thomas Coleman, who developed an elegant model to demonstrate the pressure-natriuresis phenomenon.[1–3] Since then, additional models have been developed and extended that have contributed to a deeper understanding of renal function.[4–15] Each has distinct advantages, but their utilization in drug development has been limited. Some describe nephron function in exquisite detail, but cannot dynamically link renal function with systemic sodium (Na) and volume control, thus limiting the ability to link changes in renal function with clinical measures like blood pressure. Others rely on phenomenological relationships, limiting the ability to evaluate the impact of specific mechanistic changes. Others have not been fully described publicly, making it difficult for others to evaluate and utilize them.

Here we present a model of renal physiology and systemic volume regulation that draws from previous models,[1,5,11,16–18] and which we hope will be useful in establishing a collaborative integrated model of renal function. The model facilitates dynamic simulation of systemic and renal hemodynamics through a mechanistic representation of renal filtration, reabsorption, and systemic Na and water balance. The model code is made publicly available. In a companion article, we present a case study using the model to explore mechanisms of salt-sensitive hypertension and differential responses to antihypertensive treatment in salt-sensitive and salt-resistant patients.

MATERIALS AND METHODS
Model scope
The model describes key physiological processes involved in renal function and its role in maintaining Na and water homeostasis, at the systems level, based on governing physiological and feedback mechanisms (**Figure 1**). The model is not meant to be an exhaustive molecular to organ level model, but rather, to provide a backbone for further investigation. We first describe modeling of basic renal and cardiovascular functions, based on knowledge of physical and physiological principles and morphology. We then describe key regulatory mechanisms that maintain homeostasis in the presence of perturbations, including intrinsic mechanisms like tubuloglomerular feedback (TGF) and neurohormonal mechanisms like the renin angiotensin aldosterone system (RAAS). Lastly, we describe how key parameters and setpoints were determined.

Renal function
The kidney is modeled as a set of N nephrons, each with a glomerulus (consisting of an afferent arteriole, glomerular capillaries, and efferent arteriole in series) and tubule, consisting of the proximal tubule (PT), loop of Henle (LoH), distal convoluted tubule (DCT), and connecting tubule and collecting duct (CNT/CD) (**Figure 1,** top and bottom left). In reality, after the DCT, multiple tubules coalesce into a series of collecting ducts, but the model does not attempt to capture this morphologic complexity.

Renal vasculature. The glomeruli are modeled in parallel, and in series with the preafferent (interlobar, interlobular, and arcuate arterioles) and peritubular vasculature (**Figure 1**, top left). Glomerular capillary resistance is assumed negligible. Thus, renal vascular resistance RVR is given by:

$$RVR = R_{preaff} + \frac{(R_{aa} + R_{ea})}{N_{nephrons}} + R_{peritubular} \tag{1}$$

R_{preaff} and $R_{peritubular}$ are lumped resistances describing the total resistance of preafferent and peritubular vasculatures, respectively, while R_{aa} and R_{ea} are the resistances of a single afferent or efferent arteriole, as determined from Pouiselle's law, based on the arteriole's diameter d, length L, and blood viscosity μ:

$$R_{aa} = \frac{128\mu L_{aa}}{\pi d_{aa}^4}; \quad R_{aa} = \frac{128\mu L_{ea}}{\pi d_{ea}^4} \tag{2}$$

$N_{nephrons}$ is the number of nephrons. All nephrons are assumed identical, and the model does not account for spatial heterogeneity.

Renal blood flow (RBF) is a function of the pressure drop across the kidney and RVR, according to Ohm's law:

$$RBF = \frac{MAP - P_{renal-vein}}{RVR} + \frac{GFR\left(\frac{R_{ea}}{N_{nephrons}}\right)}{RVR} \tag{3}$$

Renal venous pressure ($P_{renal-vein}$) is treated as a constant. The second term in this equation accounts for lower flow through the efferent arterioles due to GFR. As an approximation, all filtrate is assumed reabsorbed back into the peritubular capillaries, so that peritubular flow is the same as afferent flow.

Glomerular filtration. Single nephron glomerular filtration rate (SNGFR) is defined according to Starling's equation, where K_f is the glomerular ultrafiltration coefficient, P_{gc} is glomerular capillary hydrostatic pressure, P_{Bow} is pressure in the Bowman's space, and π_{go-avg} is average glomerular capillary oncotic pressure.

$$SNGFR = K_f\left(P_{gc} - P_{Bow} - \pi_{go-avg}\right) \tag{4}$$

$$GFR = SNGFR * N_{nephrons} \tag{5}$$

P_{gc} is determined according to Ohm's law:

$$P_{gc} = MAP - RBF * (R_{preaff} + R_{aa}/N_{nephrons}) \tag{6}$$

Determination of P_{Bow} and π_{go-avg} are described in the **Supplement**.

Tubular Na and water reabsorption and flow rates. The PT reabsorbs a constant fraction of filtered Na load—the glomerulotubular balance phenomenon. Na reabsorption along the PT involves multiple transporters whose expression
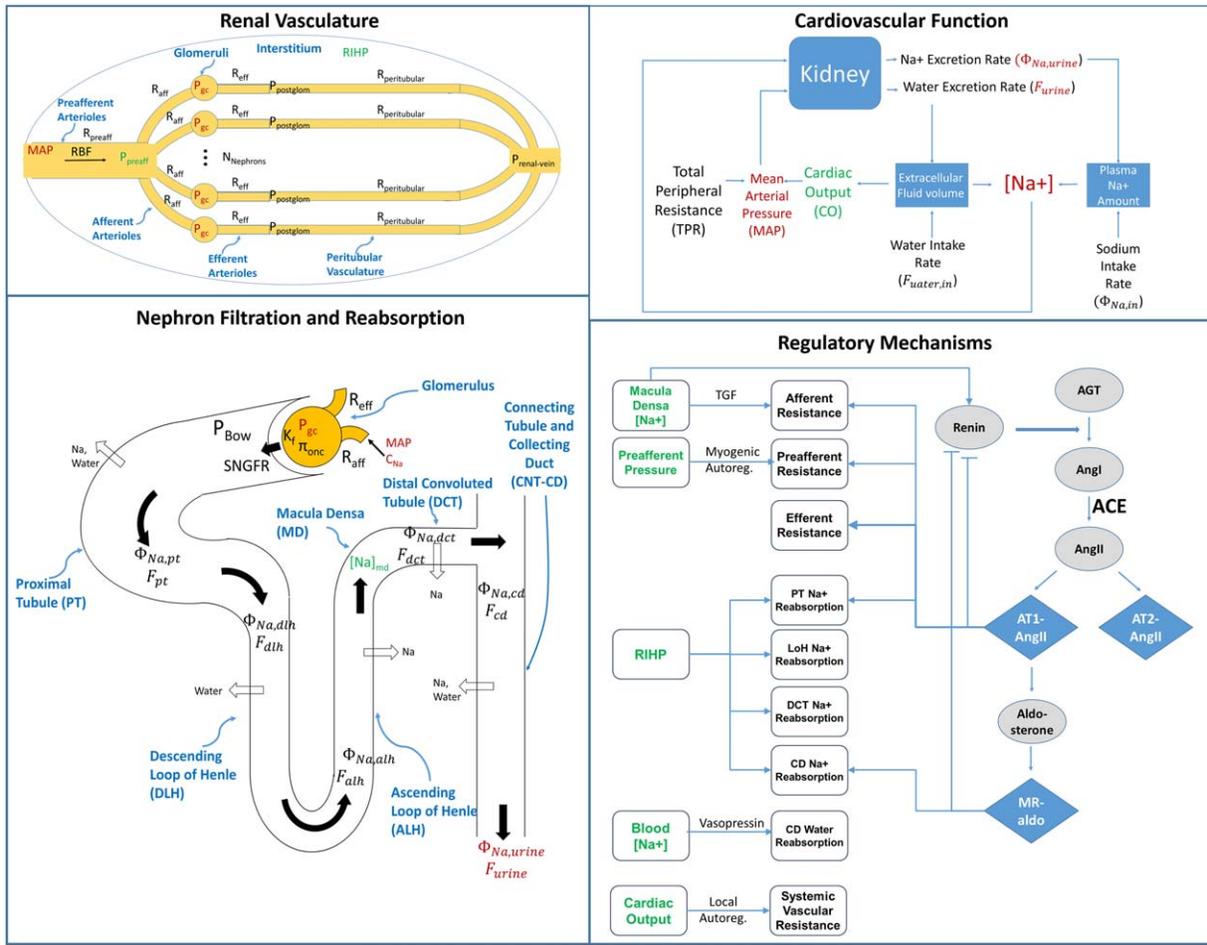
Figure 1 Schematic representation of the model. Top left: The renal vasculature is modeled by a single preafferent resistance vessel flowing into N parallel nephrons. Bottom left: Sodium and water filtration through the glomerulus is modeled according to Starling's law. Sodium and water are reabsorbed at different fractional rates in the PT, LoH, DCT, and CNT/CD, and sodium and water excretion rates are determined from unabsorbed sodium and water. Top right: Sodium and water excretion feed into the cardiovascular portion of the model, where the balance between excretion and intake determines extracellular fluid volume, plasma sodium concentration, and ultimately cardiac output and MAP. Na concentration and MAP feed back into the renal model (left), closing the loop. Bottom right: Regulatory feedback mechanisms include the RAAS, TGF, myogenic autoregulation, RIHP regulation of tubular Na+ reabsorption, vasopressin regulation of tubular water reabsorption, and local blood flow autoregulation. Variables that provide functional links between the model components are shown in red. Variables that are sensed and drive feedback mechanisms are shown in green.

varies across the different PT segments. We approximate PT Na reabsorption as homogenous along its length, so that the reabsorption rate per unit length R_{pt} is related to the fractional rate of PT Na reabsorption η_{pt} and PT length L_{pt} by:

$$R_{pt} = -\frac{\ln(1-\eta_{pt})}{L_{pt}} \quad (7)$$

Then Na flow along the length of the tubule is:

$$\Phi_{Na,pt}(x) = \Phi_{Na,pt}(0) * e^{-R_{pt}x} \quad (8)$$

$\Phi_{Na,pt}(0)$ is the filtered Na load, or the product of SNGFR and plasma Na concentration C_{Na}.

Water is reabsorbed isoosmotically in the PT, so that flow rate along the PT is:

$$F_{pt}(x) = SNGFR * e^{-R_{pt}x} \quad (9)$$

While the PT exhibits glomerulotubular balance, the degree of transport flow-dependence in distal segments is less well established, although there is evidence of flow-dependence in each segment.[19–22] To accommodate this uncertainty, the rate of reabsorption per unit length for each distal segment is formulated so that flow-dependence can be varied. For a given segment, the nominal rate of reabsorption per unit length $R_{i,0}$ is:

$$R_{i,o} = \frac{\eta_i \Phi_{Na,io}(0)}{L_i} \quad (10)$$

where η is the baseline fractional rate of reabsorption, $\Phi_{Na,0}(0)$ is the amount delivered to the segment under baseline conditions, and L is the segment length. Here i is the ascending LoH, DCT, or CNT/CD.

The actual reabsorption rate per unit length R_i is then the nominal rate $R_{i,0}$ augmented by a flow-dependent component. For B = 0, there is no flow dependence; for B = 1, changes in reabsorption are directly proportional to flow. Based on experimental data, we use a value of 0.85 for LoH,[23] and 1 for the DCT and CNT/CD.[19–22]

$$R_i = R_{i,o} + \frac{B_i \eta_i (\Phi_{Na,i}(o) - \Phi_{Na,io}(0))}{L_i} \qquad (11)$$

Na flow along each segment is then:

$$\Phi_{Na,i}(x) = \Phi_{Na,i}(0) - R_i x \qquad (12)$$

Urine Na excretion is:

$$\Phi_{Na,urine} = \Phi_{Na,cd}(L_{cd}) * N_{nephrons} \qquad (13)$$

In the LoH, water is reabsorbed in the water-permeable descending LoH (DLH) due to the osmotic gradient created by active pumping of Na out of the water-impermeable ascending limb (ALH). To model this countercurrent mechanism, we borrow from Hoppensteadt and Peskin.[18] The highly permeable DLH is assumed to quickly equilibrate with the interstitium. We also assume that all reabsorbed water and Na is picked up by the peritubular capillaries locally, and that Na follows water into the peritubular capillaries at its local concentration. With these assumptions, the Na concentration along the length of the DLH ($C_{Na,DLH}$) and in the surrounding interstitium (C_{IS}) is[18]:

$$C_{Na,DLH}(x) = C_{IS}(x) = C_{Na,DLH}(0) * e^{\left(\frac{R_{ALH}x}{F_{DLH}(0)C_{Na,DLH}(0)} \right)} \qquad (14)$$

$C_{Na,DLH}(0)$ and $F_{DLH}(0)$ (the Na concentration and fluid flow rate into the DLH) are the concentration and flow rate out of the PT.

Based on mass conservation for Na, water flow rate through the DLH is:

$$F_{DLH}(x) = \frac{F_{DLH}(0)C_{Na,DLH}(0)}{C_{Na,DLH}(x)} \qquad (15)$$

Since the ALH is impermeable to water, flow through the ALH is equal to flow at the exit (x = L) of the DLH.

$$F_{ALH}(x) = F_{DLH}(L) \qquad (16)$$

The DCT is modeled as impermeable to water, such that flow through the DCT equals flow out of the ALH.

Fine regulation of water reabsorption occurs in the CNT/CD, through aquaporin channels regulated by vasopressin. Water reabsorption through aquaporin is represented as a nominal fractional rate, modulated by the normalized vasopressin level ($\mu_{vasopressin}$):

$$\eta_{water,cnt/cd} = \eta_{water,cnt/cd,o} * \mu_{vasopressin} \qquad (17)$$

Urine flow rate F_{urine} is then:

$$F_{urine} = F_{out\_dct} * N_{nephrons} * (1 - \eta_{water,cnt/cd}) \qquad (18)$$

Cardiovascular function
Renal and systemic hemodynamics are integrally linked, and many modeling questions involve understanding the systemic impact of alterations in renal function. Thus, it is necessary to connect the loop between renal function and blood volume, cardiac output, and mean arterial pressure (**Figure 1**, top right). Here we present a simplistic model of cardiac function sufficient for many research questions. For questions where a detailed representation of cardiac and vascular hemodynamics is critical, one could replace this portion with a more detailed model of cardiovascular hemodynamics (e.g., refs. 24, 25).

Systemic water and Na dynamics are modeled with a two-compartment model of blood and extracellular fluid (ECF), where exchange occurs along an Na concentration gradient. Exchange with the intracellular space is not considered. Blood Na content ($M_{Na,blood}$) is determined by the time integral of the difference between Na intake and excretion rates, as well as transfer of Na between blood and ECF along the concentration gradient.

$$\frac{d(M_{Na,blood})}{dt} = \Phi_{Na,in} - \Phi_{Na,urine} - Q_{Na}(C_{Na,blood} - C_{Na,ecf}) \qquad (19)$$

$$\frac{d(M_{Na,ecf})}{dt} = Q_{Na}(C_{Na,blood} - C_{Na,ecf}) \qquad (20)$$

Blood volume (V_b) is modeled in an analogous manner, where V_{ecf} is blood volume. The Na concentration difference between the blood and ECF drives the transfer of water between compartments. Intracellular fluid volume is treated as a constant.

$$\frac{d(V_b)}{dt} = F_{water,in} - F_{urine} - Q_{water}(C_{Na,ecf} - C_{Na,blood}) \qquad (21)$$

$$\frac{d(V_{ecf})}{dt} = Q_{water}(C_{Na,ecf} - C_{Na,blood}) \qquad (22)$$

The blood and ECF Na concentrations ($C_{Na,blood}$ and $C_{Na,ecf}$) are then given by:

$$C_{Na,blood} = M_{Na,blood}/V_b \qquad (23)$$

$$C_{Na,ecf} = M_{Na,ecf}/V_{ecf} \qquad (24)$$

The mean cardiac filling pressure (P_{mf}) is a function of blood volume and venous compliance c_{venous}.

$$P_{mf} = P_{mf,o} + \frac{V_b - V_{b,o}}{c_{venous}} \qquad (25)$$

Cardiac output (CO) is mean filling pressure divided by resistance to venous return (R_{vr}).

$$Co = \frac{P_{mf}}{R_{vr}} \qquad (26)$$

Total peripheral resistance (TPR) is determined by treating systemic and renal vasculatures as parallel resistances, in series with venous resistance:

$$TPR = SVR * \frac{RVR}{SVR + RVR} + R_{venous} \qquad (27)$$

According to Ohm's law, mean arterial pressure (MAP) is then:

$$MAP = CO * TPR \qquad (28)$$

Regulatory mechanisms

The above equations describe physical processes of renal function, but do not explain how the kidney and cardiovascular system maintain homeostasis in the face of perturbations. Multiple control mechanisms act on the system to allow simultaneous control of C_{na}, CO, MAP, glomerular pressure, and RBF. **Figure 1** (bottom right) illustrates the regulatory mechanisms included in the model. For each control mechanism, the feedback signal μ is modeled by one of two functional forms. The choice of functional form is determined by whether a steady-state error is allowed in the controlled variable X. When a steady-state error is not allowed (i.e., X always eventually returns to the setpoint X_0), the effect is defined by a proportional-integral (PI) controller. The initial feedback signal is proportional to the magnitude of the error $(X-X_0)$, with gain G. But the feedback continues to grow over time as long as any error exists, until the error returns to zero. The integral gain K_i determines the speed of return to steady state.

$$\mu = 1 + G * \left((X - X_0) + K_i * \int (X - X_0)dt \right) \qquad (29)$$

All other mechanisms, for which the controlled variable can deviate from the setpoint at steady state, are described by a logistic equation that produces a saturating response characteristic of biological signals:

$$\mu = 1 + S * \left(\frac{1}{1 + \exp\left(\frac{X - X_0}{m}\right)} - 0.5 \right) \qquad (30)$$

Here, m defines the slope of the response around the operating point, and S is the maximal response as X goes to $\pm\infty$.

Control of plasma Na concentration by vasopressin. To sustain life, plasma Na concentration must be controlled within a tight range. For a given Na intake/excretion rate, the kidney must excrete exactly the right amount of water to maintain this target concentration. This is achieved through the effects of vasopressin. Changes in plasma osmolality are sensed via osmoreceptors, stimulating vasopressin secretion, which exerts control of water reabsorption in the CNT/CD. To ensure that C_{Na} is maintained at its setpoint $C_{Na,0}$ at steady state, this process is modeled by a PI controller:

$$\mu_{vasopressin} = 1 + G_{Na-vp} * \left(C_{Na} + K_{i-vp} * \int (C_{Na} - C_{Na,0})dt \right) \qquad (31)$$

The parameters G_{Na-vp} and K_{i-vp} are gains of proportional and integral control, respectively.

Tubular pressure natriuresis. For homeostasis, Na excretion over the long term must exactly match Na intake (the principle of Na balance). Any steady-state Na imbalance would lead to continuous volume retention or loss, an untenable situation. Pressure-natriuresis,[2] wherein changes in renal

perfusion pressure (RPP) induce changes in Na excretion, ensures that Na balance is maintained.

RPP, approximated by MAP, can impact Na excretion by two mechanisms. First, it can affect the amount of Na filtered, since glomerular filtration is pressure-driven. However, glomerular pressure is normally tightly autoregulated over a wide range of MAP. Further, this would imply that a sustained change in Na intake would require a sustained change in blood pressure and GFR to return Na balance. But in most individuals, salt intake has little impact on blood pressure and GFR. The second mechanism by which pressure can affect Na excretion is through effects on tubular Na reabsorption. The existence of this pressure-natriuresis mechanism is well established,[1] but remains surprisingly poorly understood.[26,27] It may be partially achieved through neurohumoral mechanisms including the RAAS, but there is also an intrinsic pressure-mediated effect on tubular Na reabsorption, where renal interstitial hydrostatic pressure (RIHP) is believed to be the driving signal.[28] Exactly how RIHP induces changes in tubular Na transport is not well understood, but may be mediated by Starling forces,[29] or changes in Na transporters[30] mediated by local or systemic factors.[27,31–35] Currently, we model a direct effect of RIHP on Na reabsorption in each tubular segment, without attempting to prescribe the mechanisms by which RIHP is sensed and produces changes in Na reabsorption.

RIHP is a function of peritubular capillary pressure, and particularly the vasa recta,[36,37] according to Starling's law. Pressure in the peritubular capillaries is calculated according to Ohm's law:

$$P_{peritubular} = MAP - RBF * \left(R_{preaff} + \frac{R_{aff} + R_{eff}}{N_{nephrons}} \right) \qquad (32)$$

As a simplification, we assume an increase in peritubular pressure will generate a proportional increase in RIHP. Since the kidney is encapsulated, we assume interstitial pressure equilibrates and changes in one region are transduced across the kidney. The relationship between RIHP and fractional Na reabsorption rate of each tubular segment is then modeled as:

$$\eta_{i-sodreab} = \eta_{i-sodreab,0} * \left(1 + S_{P-N,i} * \left(\frac{1}{1 + \exp(RIHP - RIHP_0)} \right) \right) \qquad (33)$$

where i = PT, LoH, DCT, or CNT/CD. $\eta_{i-sodreab,0}$ is the nominal fractional rate of reabsorption for that tubule segment. $RIHP_0$ defines the setpoint pressure and is determined from RIHP at baseline for normal Na intake. $S_{P-N,i}$ defines the maximal signal as RIHP goes to ∞.

Control of cardiac output. CO, which describes total blood flow to body tissues, returns to normal over days to weeks following a perturbation.[38] CO regulation is a complex phenomenon that occurs over multiple time scales, but we focus only on long-term control (days to weeks), which is thought to be achieved through whole-body autoregulation—the intrinsic ability of organs to adjust their resistance to maintain constant flow.[38] The total effect of local autoregulation of all organs is that TPR is adjusted to

Table 1 Parameters with values that are known from human physiology

Parameter	Definition	Normal range	Value	Units
$C_{Na,0}$	Target sodium concentration	135-145	140	mEq/L
CO_0	Cardiac output setpoint	4-8	5	L/min
C_{prot}	Plasma protein concentration	6-8	7	g/dl
c_{venous}	Venous compliance	100-150	135	mmHg/L
$d_{aff,0}$	Baseline afferent diameter	1.2-1.8	1.5	μm
$d_{eff,0}$	Baseline efferent diameter	0.9-1.2	1.1	μm
$D_{c,\ cd}$	Effective CNT/CD diameter	15-20	17	μm
D_{c_dt}	DCT tubule diameter	15-20	17	μm
D_{c_loh}	LoH diameter	15-20	17	μm
D_{c_pt}	PT diameter	20-35	27	μm
$F_{water-in}$	Water intake rate	1-3	2	L/day
K_f	Glomerular ultrafiltration coefficient	3-5	3.9	nl/min-mmHg
L_{cd}	Length of the CNT/CD	8-15	10	mm
L_{dt}	Distal tubule length	4-6	5	mm
L_{loh_asc}	Ascending LoH length	8-15	10	mm
L_{loh_des}	Descending LoH length	8-15	10	mm
L_{pt}	PT length	10-20	14	mm
MAP_0	Mean arterial pressure setpoint	80-95	85	mmHg
$N_{nephrons}$	Number of nephrons	$\sim$2e6	2.00E+06	
$P_{c\_asc\_loh}$	Ascending LoH control pressure	6-8	7	mmHg
P_{c_cd}	CNT/CD control pressure	4-6	5	mmHg
$P_{c\_des\_loh}$	Descending LoH control pressure	7-10	8	mmHg
P_{c_dt}	DCT control pressure	5-7	6	mmHg
P_{c_pt}	PT control pressure	15-22	19.4	mmHg
P_{venous}	Venous pressure	3-8	4	mmHg
RBF_0	Nominal renal blood flow	800-1,200	1,000	ml/min
$R_{preaff,0}$	Baseline preafferent resistance	10-20	14	mmHg-min/L
R_{vr}	Resistance to venous return	1-2	1.3	mmHg/min/L
β	Tubular compliance	0.2-0.4	0.2	
μ_{blood}	Blood viscosity	5.00E-07	5.00E-07	mmHg-min
η_{dt}	Nominal DCT fractional sodium reabsorption rate	0.4-0.6	0.5	
η_{loh}	Nominal LoH fractional sodium reabsorption rate	0.5-0.9	0.88	
η_{pt}	Nominal PT fractional sodium reabsorption rate	0.5-0.9	0.7	
$\Phi_{Na,in}$	Sodium intake rate	50-200	100	mmol/day

maintain CO at a constant resting level. The feedback between CO and TPR is modeled with a PI controller, such that CO is controlled to its steady-state setpoint CO_0.

$$TPR = TPR_0 * \left(1 + G_{co-tpr} * (CO + K_{i-tpr} * \int (CO - CO_0) dt) \right) \quad (34)$$

Tubuloglomerular feedback and myogenic autoregulation. TGF helps stabilize tubular flow by sensing Na concentration in the macula densa (the MD sits between the LoH and DCT; **Figure 1**, bottom left) and providing a feedback signal to inversely change afferent arteriole diameter. The preglomerular vasculature also responds to changes in perfusion pressure through myogenic vasoconstriction. Together, TGF and myogenic autoregulation exert regulatory effects on glomerular pressure and thus on GFR. Modeling of these mechanisms is described in the **Supplement.**

Renin angiotensin aldosterone system (RAAS). The RAAS is an important regulator of renal physiology, and is also implicated in many kidney-related diseases. Multiple classes of drugs for treating hypertension and kidney disease act through the RAAS. To facilitate modeling of the effects of these drugs alone and in combination, this pathway is modeled in some detail (**Figure 1,** bottom right). This pathway model[39] and physiologic effects of the RAAS[17] have been described previously. The key equations are provided in the **Supplementary Material.**

Model parameterization
Model parameters can be grouped into three categories: 1) parameters whose normal range is known from human physiology, 2) parameters that can be calculated from other parameters and known steady-state values of functional variables, and 3) fitting parameters whose values are unknown, but can be estimated based on system responses to perturbation. **Table 1** lists parameters whose normal range is known, and the values used for simulations presented here and in the companion article. This includes parameters for renal morphologic properties (e.g., number of nephrons, glomerular

Table 2 Parameters defining the RAAS pathway[17]

Parameter	Definition	Value	Units
$A_{aldo-renin}$	Strength of aldosterone negative feedback on renin secretion	−0.1	
$A_{AT1-renin}$	Strength of AT1-bound AngII negative feedback on renin secretion	−1.2	
A_{md-ren}	Strength of effect of MD sodium flow on renin secretion	1.25	
ACE	ACE rate of conversion of AngI to AngII	48.9	hr^{-1}
$Aldo_0$	Baseline aldosterone concentration	85	mg/dl
$AT1\text{-}bound\_AngII_0$	Baseline AT1-bound AngII	16.6	fmol/ml
C_{AT1}	AT1 receptor binding rate	12.1	hr^{-1}
C_{AT2}	AT2 receptor binding rate	4	hr^{-1}
Chymase	Chymase rate of conversion of AngI to AngII	1.25	hr^{-1}
$K_{d,AngI}$	AngI degradation rate	83.2	hr^{-1}
$K_{d,AngII}$	AngII degradation rate	63	hr^{-1}
$K_{d,AT1}$	AT1-bound AngII degradation rate	3.47	hr^{-1}
$K_{d,renin}$	Renin degradation rate	4	pg/ml/min
$SEC_{renin,0}$	Baseline renin secretion rate	63	pg/ml/min
PRC(0)	Baseline plasma renin concentration	62.9	pg/ml

ultrafiltration coefficient, tubular dimensions) and functional parameters (e.g., normal plasma Na concentration, CO, water and Na intake). A few parameters (SVR_0, RVR_0, $R_{peritubular}$, $\eta_{CNT/CD}$) were calculated based on values and setpoints for other parameters, as described in the **Supplement.**

The RAAS pathway parameters have been described in detail previously.[39] In short, parameters were determined in a similar way as described above—some parameter values are well known from the literature, and others were calculated to give values of RAAS peptides that fall within the observed range. The list of parameters is given in **Table 2,** and the reader is referred to previous publications for further details.

The last set of parameters are fitting constants (**Table 3**). Parameters describing the TGF response were chosen to give a fractional compensation in GFR in the range of 0.4–0.6 for a change in MD flow, as reported experimentally.[40] Rate constants for water and Na transfer between the ECF and blood were chosen so that equilibrium happens nearly instantaneously. Determination of the physiologic effects of AT1-bound AngII and aldosterone were determined based on observed changes in PRA, PRC, and blood pressure in

Table 3 Fitting parameters

Parameter	Definition	Value
G_{CO-tpr}	Cardiac output autoregulation gain	2
$G_{Na-vasopressin}$	Vasopressin controller gain	1
K_{i_vp}	Integral gain for vasopressin controller	0.1
K_{i-tpr}	Integral gain for systemic vascular resistance controller	100
m_{AT1}	Slope of AT1-bound AngII physiological effects	7
m_{aldo}	Slope of aldosterone physiological effects	0.5
$m_{autoreg}$	Preafferent myogenic autoregulation signal slope	2
m_{TGF}	TGF effect slope	0.5
Q_{Na}	Rate constant – sodium transfer between blood and ECF	1
Q_{water}	Vasopressin controller gain	1
$S_{aldo,CD}$	Max effect on CD reabsorption as aldosterone goes to infinity	0.3
$S_{aldo,DCT}$	Max effect on DCT reabsorption as aldosterone goes to infinity	0.1
$S_{AT1,aff}$	Max effect on preafferent resistance as AT1-bound AngII goes to infinity	0.5
$S_{AT1,aldo}$	Max effect on aldosterone as AT1-bound AngII goes to infinity	0.05
$S_{AT1,eff}$	Max effect on efferent resistance as AT1-bound AngII goes to infinity	0.3
$S_{AT1,preaff}$	Max effect on afferent resistance as AT1-bound AngII goes to infinity	0.5
$S_{AT1,PT}$	Max effect on PT sodium reabsorption as AT1-bound AngII goes to infinity	0.1
$S_{AT1,sys}$	Max effect on systemic resistance as AT1-bound AngII goes to infinity	0.02
$S_{autoreg}$	Max myogenic autoregulatory effect on preafferent resistance	0.5
S_{TGF}	TGF maximal response as Φ_{md-sod} goes to infinity	0.6
$S_{P-N,LoH}$	Max effect on LoH sodium reabsorption as RIHP goes to infinity	3
$S_{P-N,CD}$	Max effect on CNT/CD sodium reabsorption as RIHP goes to infinity	3
$S_{P-N,DCT}$	Max effect on DCT sodium reabsorption as RIHP goes to infinity	3
$S_{P-N,PT}$	Max effect on PT sodium reabsorption as RIHP goes to infinity	3

Table 4 Comparison of simulated steady-state output variables with known ranges for human physiology

Variable	Normal range	Value	Units
SVR	0-20	16.8	mmHg-L/min
CO	4-8	5	L/min
MAP	80-95	84	mmHg
RVR	65-120	80.8	mmHg-L/min
RBF	800-1200	999	ml/min
RPF	450-750	594	ml/min
Glomerular Pressure	55-62	60	mmHg
FPR	50-78	69.8	%
FDR	95-99	98.2	%
FENa	0.5-2	0.5	%
Filtration Fraction	15-20	16.9	%
GFR	90-120	100	ml/min
SNGFR	45-60	50	nl/min
Bowman Pressure	15-22	19.6	mmHg
Na concentration	135-150	140	mEq/L
MD sodium concentration	40-80	61	mEq/L
24 hr urine volume		2.1	L/day
24 hr Na excretion		100	mEq/day
Aldosterone	40-150	86.4	pg/ml
PRA	0.2-3.3	1.02	ng/ml/hr
PRC	3-50	16.8	pg/ml
blood volume	3.5-7	4.95	L
extracellular fluid volume	13-18	15	L

response to therapies targeting the RAAS, as described previously.[17] In the next section, we explore the impact of parameter choices for the PI controllers of Na concentration (Eq. 31, $G_{Na-vasopressin}$ and K_{i-vp}) and CO (Eq. 34, G_{CO-tpr} and K_{i-tpr}).

The pressure natriuresis mechanism, modeled through effects of RIHP on tubular reabsorption ($S_{P-N,i}$), plays a critical role in regulating blood pressure, and impairment in this mechanism may contribute to salt-sensitive hypertension and alterations in renal hemodynamics. In the companion article, we explore in depth the impact of parameter choice for this feedback mechanism.

Software implementation

The model was implemented in a free open-source programming software (R 3.1.2). It utilizes the RxODE package.[41] Model code is provided in the **Supplement,** and is also available on Github at https://github.com/hallowkm/RenalModel.

RESULTS

Comparison of model steady-state outputs with clinically observed measures

Table 4 shows the simulated steady-state output of key renal and cardiovascular variables for which normal ranges are known from the literature. All model variables fall within the observed ranges.

Modeling of feedback control and homeostasis

A critical feature of the cardiorenal system is the ability to restore homeostasis after perturbations. Under normal physiologic conditions, plasma Na concentration (C_{Na}), blood pressure, and blood flows (CO and RBF) are maintained at stable levels. Under pathophysiological conditions (hypertension, kidney injury, cardiac dysfunction), control of variables that are less critical to life (e.g., blood pressure, RBF) may be sacrificed at the expense of the most critical—C_{Na} and CO. Drugs that act by perturbing renal Na handling or blood volume/CO will invoke these feedback mechanism. Thus, any model seeking to describe the long-term renal and systemic hemodynamic response to therapies must be able to describe the return of C_{Na} and CO to their setpoint after perturbation.

Control of C_{Na} is achieved through the action of vasopressin on water reabsorption in the CNT/CD, allowing water excretion to be decoupled from Na excretion. We used a PI controller as a mathematical construct to represent this complex and incompletely understood process. The gains of this controller must be chosen to reproduce the ultimate effect of this mechanism: maintenance of C_{Na} at equilibrium levels (±1 mmol/L) after a perturbation such as an increase in Na intake.[42,43] **Figure 2a** shows the C_{Na} response to a step change (doubling) in Na intake, for different controller gains. When no integral controller is
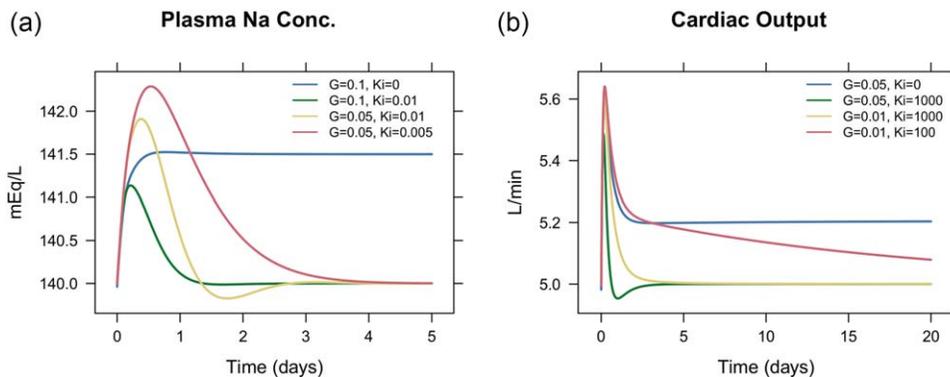

Figure 2 Impact of choice of controller gains for proportional-integral feedback controllers on the response of cardiac output (**a**) and Na concentration (**b**) to a perturbation (step increase in Na intake). Gains were chosen so that these variables quickly returned to steady state without oscillations (yellow lines).

included ($K_{i-vp} = 0$), a change in Na intake produces a steady-state error in C_{Na}, and the size of this error varies inversely with G_{Na-vp}. Introducing the integral controller ($K_{i-vp} > 0$) ensures that there is no steady-state error. The magnitude of the integral gain K_{i-vp} determines the speed at which the system returns to steady state. However, if K_{i-vp} is made too large relative to the proportional gain G, oscillations result. Thus, values for proportional and integral gain were set so that after a perturbation, C_{Na} deviated less than 1 mmol/L and returned to the setpoint without overshoot.

Control of CO, achieved physiologically through changes in whole-body resistance over days to weeks in response to changes in tissue blood flow throughout the body,[38] was modeled similarly. **Figure 2b** shows the simulated CO response to a step increase in Na intake, for different controller gains. When no integral controller is included ($K_{i-tpr} = 0$), a perturbation produces a steady-state error in CO and this is inversely proportional to the value of the proportional gain (G_{CO-tpr}). Including an integral controller ($K_{i-vp} > 0$) eliminates the steady-state error, and the magnitude of the integral gain determines the speed at which the system returns to steady state. Thus, values for proportional and integral gain were set so that after a perturbation, cardiac output returned to the setpoint over a few days without overshoot, as is observed experimentally.[38]

DISCUSSION

Here we presented a model of renal function and systemic hemodynamics that may serve as a starting point for many systems pharmacology applications in renal and cardiovascular disease. The model equations, code, and parameters are made fully available for review and use. We believe that a common open-source model is an important starting point for advancing the use of QSP modeling in renal physiology, pharmacology, and drug development.

The model draws from previously published models, and incorporates core components of renal function and control necessary to model most problems related to renal function. The key strengths of the model are that it integrates a mechanistic representation of kidney filtration and reabsorption with systemic control of Na and water homeostasis, and allows simulation of key clinical endpoints: GFR, MAP, Na excretion, RAAS biomarkers, etc. The model is not an exhaustive description of renal physiology, but rather provides a starting point that can be refined as needed to address new questions. For instance, representation of PT transport could be refined if one wished to model a particular transport inhibitor. Neurohormonal feedbacks could be refined or represented in greater detail as needed to model effects of a treatment targeting that pathway. The vascular and cardiac representation in the model could be expanded, for instance, to address questions related to the renal effects on heart failure.

In a companion article, we describe the application of this model to test hypotheses regarding mechanisms of salt-sensitive hypertension and the differential response to antihypertensive therapy in salt-resistant compared to salt-sensitive subjects.

1. Guyton, A.C., Coleman, T.G. & Granger, H.J. Circulation: overall regulation. *Annu. Ref. Physiol.* **34**, 13–46 (1972).
2. Guyton, A.C. *et al.* A systems analysis approach to understanding long-range arterial blood pressure control and hypertension. *Circ. Res.* **35**, 159–176 (1974).
3. Guyton, A.C. Long-term arterial pressure control: an analysis from animal experiments and computer and graphic models. *Am. J. Physiol.* **259**, R865–877 (1990).
4. Roy, D.R., Layton, H.E. & Jamison, R.L. *Countercurrent Mechanism and Its Regulation. The Kidney: Physiology and Pathophysiology*, 3rd edn (Lippincott Williams & Wilkins, Philadelphia, 2000).
5. Karaaslan, F., Denizhan, Y., Kayserilioglu, A. & Gulcur, H.O. Long-term mathematical model involving renal sympathetic nerve activity arterial pressure, and sodium excretion. *Ann. Biomed. Eng.* **33**, 1607–1630 (2005).
6. Averina, V.A., Othmer, H.G., Fink, G.D. & Osborn, J.W. A new conceptual paradigm for the haemodynamics of salt-sensitive hypertension: a mathematical modelling approach. *J. Physiol.* **590**, 5975–5992 (2012).
7. Beard, D.A. & Mescam, M. Mechanisms of pressure-diuresis and pressure-natriuresis in Dahl salt-resistant and Dahl salt-sensitive rats. *BMC Physiol.* **12**, 6 (2012).
8. Moss, R. & Layton, A.T. Dominant factors that govern pressure natriuresis in diuresis and antidiuresis: a mathematical model. *Am. J. Physiol. Renal Physiol.* **306**, F952–969 (2014).
9. Weinstein, A.M. A mathematical model of the rat proximal tubule. *Am. J. Physiol.* **250**, F860–873 (1986).
10. Weinstein, A.M. *et al.* Flow-dependent transport in a mathematical model of rat proximal tubule. *Am. J. Physiol. Renal Physiol.* **292**, F1164–1181 (2007).
11. Weinstein, A.M. A mathematical model of rat proximal tubule and loop of Henle. *Am. J. Physiol. Renal Physiol.* **308**, F1076–1097 (2015).
12. Edwards, A. & Layton, A.T. Nitric oxide and superoxide transport in a cross section of the rat outer medulla. I. Effects of low medullary oxygen tension. *Am. J. Physiol. Renal Physiol.* **299**, F616–633 (2010).
13. Layton, A.T. A mathematical model of the urine concentrating mechanism in the rat renal medulla. I. Formulation and base-case results. *Am. J. Physiol. Renal Physiol.* **300**, F356–371 (2011).
14. Layton, A.T., Vallon, V. & Edwards, A. Modeling oxygen consumption in the proximal tubule: effects of NHE and SGLT2 inhibition. *Am. J. Physiol. Renal Physiol.* **308**, F1343–1357 (2015).
15. Hester, R.L. *et al.* HumMod: A Modeling environment for the simulation of integrative human physiology. *Front. Physiol.* **2**, 12 (2011).
16. Jensen, P.K., Christensen, O. & Steven, K. A mathematical model of fluid transport in the kidney. *Acta Physiol. Scand.* **112**, 373–385 (1981).
17. Hallow, K.M. *et al.* A model-based approach to investigating the pathophysiological mechanisms of hypertension and response to antihypertensive therapies: extending the Guyton model. *Am. J. Physiol. Regul. Integr. Comp. Physiol.* **306**, R647–662 (2014).
18. Hoppensteadt, F.C., Peskin, C.S. & Hoppensteadt, F.C. *Modeling and Simulation in Medicine and the Life Sciences*, 2nd edn (Springer, New York, 2002).
19. Kunau, R.T., Jr., Webb, H.L. & Borman, S.C. Characteristics of the relationship between the flow rate of tubular fluid and potassium transport in the distal tubule of the rat. *J. Clin. Investig.* **54**, 1488–1495 (1974).
20. Satlin, L.M., Sheng, S., Woda, C.B. & Kleyman, T.R. Epithelial Na(+) channels are regulated by flow. *Am. J. Physiol. Renal Physiol.* **280**, F1010–1018 (2001).
21. Satlin, L.M., Carattino, M.D., Liu, W. & Kleyman, T.R. Regulation of cation transport in the distal nephron by mechanical forces. *Am. J. Physiol. Renal Physiol.* **291**, F923–931 (2006).
22. Palmer, L.G. & Schnermann, J. Integrated control of Na transport along the nephron. *Clin. J. Am. Soc. Nephrol.* **10**, 676–687 (2015).
23. Vallon, V., Osswald, H., Blantz, R.C. & Thomson, S. Potential role of luminal potassium in tubuloglomerular feedback. *J. Am. Soc. Nephrol.* **8**, 1831–1837 (1997).
24. Tsuruta, H., Sato, T., Shirataka, M. & Ikeda, N. Mathematical model of cardiovascular mechanics for diagnostic analysis and treatment of heart failure: part 1. Model description and theoretical analysis. *Med. Biol. Eng. Comput.* **32**, 3–11 (1994).
25. Arts, T., Bovendeerd, P., Delhaas, T. & Prinzen, F. Modeling the relation between cardiac pump function and myofiber mechanics. *J. Biomech.* **36**, 731–736 (2003).

26. Granger, J.P., Alexander, B.T. & Llinas, M. Mechanisms of pressure natriuresis. *Curr. Hypertens. Rep.* **4**, 152–159 (2002).

27. O'Connor, P.M. & Cowley, A.W, Jr. Modulation of pressure-natriuresis by renal medullary reactive oxygen species and nitric oxide. *Curr. Hypertens. Rep.* **12**, 86–92 (2010).

28. Garcia-Estan, J. & Roman, R.J. Role of renal interstitial hydrostatic pressure in the pressure diuresis response. *Am. J. Physiol.* **256**, F63–70 (1989).

29. Schafer, J.A. Transepithelial osmolality differences, hydraulic conductivities, and volume absorption in the proximal tubule. *Annu. Ref. Physiol.* **52**, 709–726 (1990).

30. McDonough, A.A. Mechanisms of proximal tubule sodium transport regulation that link extracellular fluid volume and blood pressure. *Am. J. Physiol. Regul. Integr. Comp. Physiol.* **298**, R851–861 (2010).

31. Haas, J.A., Khraibi, A.A., Perrella, M.A. & Knox, F.G. Role of renal interstitial hydrostatic pressure in natriuresis of systemic nitric oxide inhibition. *Am. J. Physiol.* **264**, F411–414 (1993).

32. Nakamura, T. *et al.* Effects of renal perfusion pressure on renal interstitial hydrostatic pressure and Na+ excretion: role of endothelium-derived nitric oxide. *Nephron* **78**, 104–111 (1998).

33. Roman, R.J. & Lianos, E. Influence of prostaglandins on papillary blood flow and pressure-natriuretic response. *Hypertension* **15**, 29–35 (1990).

34. Mizelle, H.L., Hall, J.E. & Hildebrandt, D.A. Atrial natriuretic peptide and pressure natriuresis: interactions with the renin-angiotensin system. *Am. J. Physiol.* **257**, R1169–1174 (1989).

35. Nishimoto, M. & Fujita, T. Renal mechanisms of salt-sensitive hypertension: contribution of two steroid receptor-associated pathways. *Am. J. Physiol. Renal Physiol.* **308**, F377–387 (2015).

36. Farrugia, E., Lockhart, J.C. & Larson, T.S. Relation between vasa recta blood flow and renal interstitial hydrostatic pressure during pressure natriuresis. *Circ. Res.* **71**, 1153–1158 (1992).

37. Cowley, A.W., Roman, R.J., Fenoy, F.J. & Mattson, D.L. Effect of renal medullary circulation on arterial pressure. *J. Hypertens. Suppl.* **10**, S187–193 (1992).

38. Coleman, T.G., Granger, H.J. & Guyton, A.C. Whole-body circulatory autoregulation and hypertension. *Circ. Res.* **28**(suppl 2), 76–87 (1971).

39. Lo, A. *et al.* Using a systems biology approach to explore hypotheses underlying clinical diversity of the renin angiotensin system and the response to antihypertensive therapies. In *Clinical Trial Simulations* (ed. Peck HHCKCC), Springer, New York (2011).

40. Vallon, V., Blantz, R.C. & Thomson, S. Homeostatic efficiency of tubuloglomerular feedback is reduced in established diabetes mellitus in rats. *Am. J. Physiol.* **269**, F876–883 (1995).

41. Wang, W., Hallow, K.M. & James, D.A. A tutorial on RxODE: simulating differential equation pharmacometric models in R. *CPT Pharmacometr. Syst. Pharmacol.* **5**, 3–10 (2016).

42. Kirkendall, A.M. *et al.* The effect of dietary sodium chloride on blood pressure, body fluids, electrolytes, renal function, and serum lipids of normotensive man. *J. Lab. Clin. Med.* **87**, 411–434 (1976).

43. Heer, M., Baisch, F., Kropp, J., Gerzer, R. & Drummer, C. High dietary sodium chloride consumption may not induce body fluid retention in humans. *Am. J. Physiol. Renal Physiol.* **278**, F585–595 (2000).

Supplementary information accompanies this paper on the *CPT: Pharmacometrics & Systems Pharmacology* website (http://psp-journal.com)